POSITION PAPER

Metropolitan Area Network Model Design Using Regional Railways Information for Beyond 5G Research

Takuji TACHIBANA[†a)], *Senior Member*, Yusuke HIROTA[††b)], Keijiro SUZUKI[†††c)], *Members*, Takehiro TSURITANI[††††d)], *Fellow, and* Hiroshi HASEGAWA[†††††e)], *Senior Member*

SUMMARY   To accelerate research on Beyond 5G (B5G) technologies in Japan, we propose an algorithm that designs mesh-type metropolitan area network (MAN) models based on a priori Japanese regional railway information, because ground-truth communication network information is unavailable. Instead, we use the information of regional railways, which is expected to express the necessary geometric structure of our metropolitan cities while remaining strongly correlated with their population densities and demographic variations. We provide an additional compression algorithm for use in reducing a small-scale network model from the original MAN model designed using the proposed algorithm. Two Tokyo MAN models are created, and we provide day and night variants for each while highlighting the number of passengers alighting/boarding at each station and the respective population densities. The validity of the proposed algorithm is verified through comparisons with the Japan Photonic Network model and another model designed using the communication network information, which is not ground-truth. Comparison results show that our proposed algorithm is effective for designing MAN models and that our result provides a valid Tokyo MAN model.
key words: metropolitan area network, Beyond 5G, regional railway, network model design, Tokyo metropolitan area

1. Introduction

The fifth generation (5G) of wireless communication promises to fulfil several new service and enterprise requirements, such as ultra-high speed, low latency, and multiple simultaneous connections. Metropolitan area networks (MANs) are expected to be the key to implementing such 5G services [1]–[4] and will become more important in the forthcoming "Beyond 5G" (B5G) era [5]. The research and development of network technologies and systems aiming for B5G must be conducted using appropriate MAN mod-

(a) Topology with multiple rings.

(b) Undirected graph with no self-loops and no multiple edges.
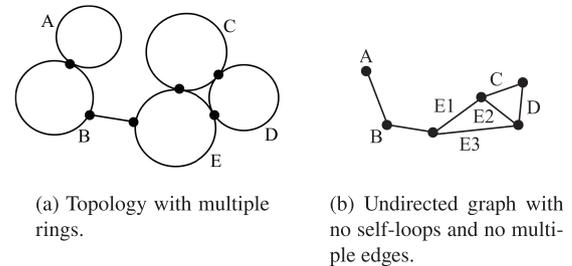
Fig. 1   Relationship between topology with multiple rings and undirected graph with no self-loops and no multiple edges.

els, and their network-level performances must be verified based on the specific metropolitan characteristics and geography. These characteristics must be parametrized as topology graphs with nodes, link lengths, and traffic distributions/intensities. Prior to this, benchmarking metrics, including the total number of facilities and transmission latency/throughput between node pairs, must be appropriately measured.

Extant MAN models from worldwide metropolitan areas are available and will greatly contribute to 5G/B5G deployment [6]–[8]. Most topologies of MANs are mesh-type and ring-type [9], and the mesh-type is currently more common than ring-type [10]. Moreover, as shown in Fig. 1, a topology with multiple rings is represented as a mesh-type topology if an undirected graph with no self-loops and no multiple edges, which are also known as parallel edges [11], has to be used in B5G research. This is because a ring is denoted as a vertex or edges depending on the number of vertexes on the ring. Hence, mesh-type MAN models are more appropriate to provide useful B5G research material. However, to the best of authors' knowledge, there are no mesh-type MAN models in Japan. One reason for this lack is that there are no ground-truth MAN data about Japan cities [12]. Moreover, it is difficult to design MAN models using current design approaches as can be inferred from the fact that no new MAN models has been created for several years. Hence, new approaches for designing mesh-type MAN models are needed to enhance B5G research in Japan.

To establish this approach, alternative information is required. Notably, a vast database of transportation infrastructure information is publicly available. Originally, communication networks were constructed by utilizing the existing social infrastructure (e.g., sewer and transportation),

and cables were installed along motorways, railway lines, and sewer pipes, not to mention the many underground cable plants [13]. Therefore, communication networks are usually well-aligned geographically with the transportation infrastructure [12], although their similarities and differences come with four interaction types: substitute, complement, modify, and neutral [14]–[20].

Japan Photonic Network Model (JPNM) that captures the core network in Japan was designed based on transportation information and regional characteristics (e.g., population distributions) because ground-truth network information was not available [21], [22]. The JPNM consists of three models that have different numbers of nodes and links. The JPNM has been used for performance evaluations in many studies and has contributed significantly to the development of network technologies [23], [24]. In summary, public information on regional railways and their characteristics is expected to be utilized to design MAN models in Japan.

In this paper, we propose an algorithm for designing mesh-type MAN models to accelerate B5G research, and it is completely different from the algorithm for designing JPNM. The algorithm utilizes information on regional railways, including topology and the number of passengers alighting and boarding at each railway station. Regional characteristics (e.g., population distributions and government office locations) are also used alongside the connectivity situations between node pairs, maximum nodal degrees, and number of nodes. We also propose a separate compression algorithm that is used to create a small-sized network model from the original larger network model designed using the first algorithm. These algorithms, which include several common and general-purpose processes, are intended for the Tokyo 23-wards metropolitan area, which is well-served by regional railways. Therefore, some aspects of the algorithms must be revised when porting to new metropolitan areas.

Using our proposed algorithms, we designed two different sized MAN models of the Tokyo 23-wards area, which is well served by regional railways. One model has 23 nodes and 43 links, and the other has 12 nodes and 21 links. Day and night versions of each are also designed using the population densities and numbers of passengers alighting/boarding at each station. We provide a thorough explanation of how we tailored the proposed algorithms to the Tokyo 23-wards area. Our four MAN models should be able to be leveraged according to their research goals and performance evaluation intentions. We investigated the efficacy and validity of our proposed algorithms by comparing our designed models with others. However, our two algorithms cannot be compared with existing approaches because previous Tokyo 23-wards MANS do not exist. Moreover, the validity of proposed algorithms cannot be discussed based on the lack of ground-truth information.

The novelty and contributions of this paper are summarized as follows:

- A MAN model design algorithm based on a priori regional railway information and regional characteristics is proposed.

- A compression algorithm is proposed for developing smaller network models from the original MAN model.

- Mesh-type MAN models of Tokyo 23-wards area are designed to accelerate research on B5G.

Our proposed MAN model-design algorithm is pioneering and innovative because only publicly available regional railway information and characteristics are used to design MAN models. The resulting Tokyo23 and Tokyo12 models are the first relevant mesh-type MAN models in the world, and B5G research in Japan are expected to be accelerated as a result.

The remainder of this paper is organized as follows. Section 2 provides an overview of the extant network modelling approaches and explains the JPNM in detail. Section 3 explains our proposed algorithm for designing MAN models, and in Sect. 4, two MAN models for the Tokyo 23-wards is designed. Section 5 explains our proposed compression algorithm for preparing a small-sized model from the original full-MAN model, and Sect. 6 describes the specific design for the Tokyo 23-wards. Section 7 presents the characteristics of the four designed network models, and the validity of our proposed algorithm is investigated in Sect. 8. Finally, Sect. 9 concludes this paper.

2. Related Work

2.1 Existing Network Model Design Approaches

In this subsection, we explain the existing approaches for designing network models.

One of the simplest approaches to network mapping is to directly use the configuration file of each internet protocol (IP) router [25], [26]. Because the configuration file includes the current operational information, a ground-truth network model can be designed using these files. However, most configuration files are not published because of their high confidentiality; hence, these materials are rarely available to researchers. The record route of the IP header can also be used as it accumulates packet routing information as it traverses the network [27]. Unfortunately, this approach cannot be used in many situations owing to security and performance concerns.

The traceroute command has been utilized to design network models in many studies [28]–[33], and its efficacy can be improved by exploiting parallel probes and stochastic sampling methods [34]. However, it is difficult to map IP router interfaces to the correct routers and trace accurate routes through opaque Layer-2 clouds [35]. The traceroute command is therefore insufficient for scientifically inferring connectivity at the IP router level. To design a statistical network model, network tomography has been utilized [36], [37]. In this approach, probe packets are sent from a source to destination nodes to measure the distances between them. Unfortunately, the large error accumulations that are normal in this method renders the method inappropriate for MANs.

When network operators make their own network information public, it becomes possible to build ground-truth

models. This was accomplished by Knight et al. [38] and Bowden et al. [39]. However, much of the network information was manually designed [38], which inherently leads to inaccuracies. This approach is also inappropriate, because most network operators do not publish detailed network information, and those that do tend to lack accuracy and validity.

Several analytical methods of designing network models have been proposed [40]. The Erdős–Rényi method [41] can be used to design a random network model, and the Watts–Strogatz method [42] is an algorithm for designing random network models with small-world properties. The Barabási–Albert method [43] is the most popular algorithm for creating scale-free network models. In addition, the Gabriel [44] and Waxman [45] methods can be used to design network models by explicitly using information on node locations. Arakawa et al. [46] proposed a design method in which a new node likely connects to the nearest one, and new links are added based on node utilization. Fabrikant et al. [47] presented a model-design method in which a newly added node connects to existing ones to minimize the sum of the Euclidian distances between them and the logical distances from existing nodes. These algorithmic methods are useful for designing general network models; however, they are ineffective when designing network models based on regional characteristics.

Thus, many network model design methods have been proposed owing to the importance of the endeavor. Nevertheless, no appropriate methods exist to create MAN models, because the ground-truth information does not exist.

2.2 Optical Core Network Model in Japan

Figure 2 shows three optical core network models in Japan: JPN48, JPN25, and JPN12 [21], [22]. In JPN48 (Fig. 2(a)), a node is placed in each prefecture, and an additional one is placed in Tokyo. Each node is named after its respective prefecture capital, and the number of degrees is greater than or equal to two. Each link between nodes is set according to the following priority order of six railway lines: 1) Shinkansen bullet-train line, 2) Japan Railways (JR) express line, 3) private railway express line, 4) JR conventional line, 5) private railway conventional line, and 6) subway line. If there is no railway line between two nodes, a regular shipping line is selected.

JPN25 consists of 25 nodes, as shown in Fig. 2(b). The model consists of 20 nodes selected in descending order based on prefectural population, four nodes selected from prefectures with Ministry of Internal Affairs of Communications (MIC) offices, and another node in Tokyo. Figure 2(c) also shows JPN12, which includes 11 nodes selected from prefectures with MIC government offices and another in Tokyo. Note that one node is located in Hakata, where the population is the largest in Kyushu; however, the MIC government office is located in Kumamoto Prefecture.

In these network models, regional population information is added to each node. The population per node is based
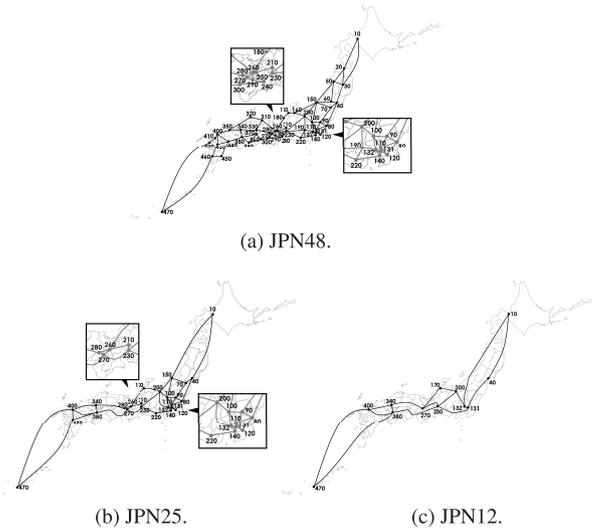

(a) JPN48.

(b) JPN25.   (c) JPN12.

Fig. 2   Three optical core network models in Japan.

on the corresponding prefecture. Each link length is determined by the route of the selected railway line or regular shipping line. Detailed information on all models can be downloaded from [48].

3. MAN Model Design Algorithm Using Regional Railway Information

In this section, we propose our method of designing MAN models using regional railway information, which is not used by any of the existing methods discussed in Sect. 2.1. The MAN model is a simple plane graph that can be tailored for many additional studies. In the following, we focus on a metropolitan area with many railway lines. The proposed algorithm includes common and general-purpose processes that can be tailored to accommodate many metropolitan areas. These processes must be revised according to the region in question. Table 1 shows the list of variables used in our proposed model-design algorithm.

In the proposed model-design method, the number of nodes, N, is given in advance, and n_i denotes the ith node ($i = 1, \cdots, N$). Here, a node corresponds to a city, ward, town, etc. in the metropolitan area. For n_i, let L_i denote the number of railway lines whose stations are in n_i, and let the jth railway, ($j = 1, \cdots, L_i$), be denoted as r_{ij}. Additionally, the number of stations for r_{ij} in n_i is S_{ij}, and the kth station is denoted as s_{ij}^k ($k = 1, \cdots, S_{ij}$). Figure 3 shows two nodes, n_i and n_j. In Fig. 3, lines r_{i1} and r_{ij} are shown in n_i, and S_{ij} is eight in n_i. The stations are denoted as s_{i1}^m and s_{ij}^k for r_{i1} and r_{ij}, respectively.

When the number of passengers alighting/boarding at s_{ij}^k is p_{ij}^k, the maximum number of passengers in n_i for r_{ij} is given by $p_{ij}^{max} = \max_k p_{ij}^k$. For N nodes, the links are set using the following algorithm:

A-1) Set $i = 1$ and go to A-2).

A-2) For n_i, select two railway lines, $r_{i\delta}$ and $r_{i\eta}$, such that

Table 1 List of variables for the proposed model-design algorithm.

Variable	Railway & characteristics information
N	Number of nodes.
n_i	ith node.
L_i	Number of railway lines for n_i.
r_{ij}	jth railway line for n_i.
S_{ij}	Number of stations in n_i for r_{ij}.
s_{ij}^k	kth station in n_i for r_{ij}.
p_{ij}^k	Number of passengers at s_{ij}^k.
p_{ij}^{max}	Maximum number of passengers at any station in n_i for r_{ij} ($\max_k p_{ij}^k$).
b_i	Population size of n_i.
s_{ij}^{max}	kth station whose p_{ij}^k is equal to p_{ij}^{max}.
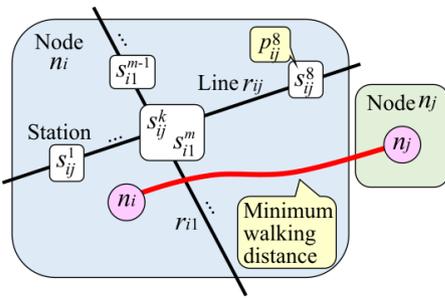
Fig. 3 Relationship among nodes, stations, and railway lines.

$p_{i\delta}^{max}$ and $p_{i\eta}^{max}$ are large. Then, go to A-3).

A-3) A link is set between n_i and n_j that is adjacent to n_i for $r_{i\delta}$. Moreover, a link is set between n_i and n_k, which is adjacent to n_i for $r_{i\eta}$. Go to A-4).

A-4) After i is increased by one, go to A-2) if i is smaller than N; otherwise, go to A-5).

A-5) When multiple links intersect at a point, a link is deleted until there are no link intersections and only one link remains. Go to A-6).

A-6) Some links are deleted for the highest-degree nodes for exception handling. Then, the algorithm is completed.

In this design algorithm, the processing order of the nodes has little effect on the designed network model. If a mesh-type MAN model cannot be designed appropriately, the processing order should be changed at A-1). In A-2), if the number of passengers is unknown for each railway line of station s_{ij}^k, then p_{ij}^k is set to $\sum_{j=1}^{L_i} p_{ij}^k$, regardless of the railway line, r_{ij}. In this case, p_{ij}^k and $p_{i\delta}^k$ are the same, and they increase when s_{ij}^k has many railway lines. If $p_{i\delta}^k$ is also not obtained, the population size of n_i may be utilized. Moreover, A-2) and A-3) ensure that a node with a larger total number of passengers has a larger number of links. In these steps, when n_i has no starting and terminal stations and is not adjacent to areas outside the MAN for $r_{i\delta}$ and $r_{i\eta}$, at most four links are set to n_i. Even if three or more

railway lines are selected for n_i, many lines are duplicates of lines selected for other nodes, and the number of links does not increase considerably. On the other hand, links are more likely to be set to nodes with non-major railway lines, such as subways. Because such nodes are often minor, some links can be deleted in A-6). In A-5), a link between two nodes with a larger distance should be deleted to support the design of a simple plane graph, which will be useful to other research areas [49]. The computational complexity of this algorithm is presented in the Appendix.

After this algorithm completes, information on the link length is set for each link based on the distances between adjacent nodes. Then, the population size is set to n_i based on the population size in the corresponding city, ward, town, etc. and the number of passengers at r_{ij}. Finally, the design of the MAN model is completed.

4. MAN Model with 23 Nodes in Tokyo

In this section, we design a MAN model with 23 nodes, "Tokyo23," referring to the design algorithm proposed in Sect. 3. Notably, Tokyo23 is classified into two models: *day* and *night* versions, based on the number of passengers alighting/boarding at each station and the respective population densities.

Figure 4 shows the designed Tokyo23 MAN model. As shown in the figure, each node is identified by the name of one of the 23 wards in Tokyo, and each node is located in a ward office building. To design Tokyo23, N was set to 23 in the proposed algorithm. In A-2), the total number of passengers, $\sum_j p_{ij}^k$, alighting/boarding at s_{ij}^k is used as p_{ij}^k, regardless of r_{ij}, because it is otherwise too difficult to obtain p_{ij}^k. The link between Taito and Kita is deleted due to its long link length so that a simple plane graph will result from A-5). Moreover, in A-6), the link between Bunkyo and Taito is deleted to reduce the node degree of Bunkyo, which has the largest degree owing to its concentration of subway lines, which are rarely selected for other nodes.

The minimum walking distance between two ward office buildings is used as the link length between corresponding nodes. Then, the population size is assigned to each node using the number of passengers alighting/boarding at each station and the respective population densities. When the population size of the ward corresponding to n_i is represented as b_i, the population size of n_i is equal to b_i for the *Tokyo23-night* model. For the *Tokyo23-day* model, if the information on daytime population, b_i^d, of the ward corresponding to n_i is obtained, b_i^d is set to the population size of n_i. Otherwise, the number of passengers alighting/boarding at each station is used. Let s_{ij}^{max} denote the station whose number of passengers is p_{ij}^{max}, which includes the passengers from/to outside the 23 wards. The population size of n_i is given by

$$\frac{b_i \sum_{j=1}^{L_i} p_{ij}^{max} x_{ij}}{\sum_{i=1}^{N} \sum_{j=1}^{L_i} p_{ij}^{max} x_{ij}}, \qquad (1)$$
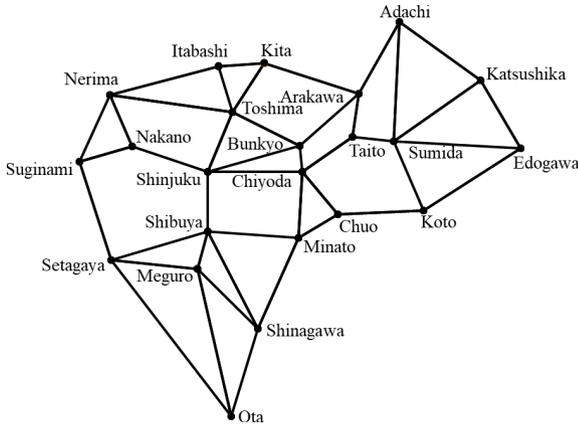
Fig. 4 Designed Tokyo23 MAN model.

Table 2 List of variables for the proposed compression algorithm.

Variable	Railway & characteristics information
N^S	Number of nodes in small-sized model.
M	Number of areas in the original model.
U_m	Set of nodes in the mth area in original model.
$|U_m|$	Number of nodes in U_m.
n_i^S	ith nodes in small-sized model.
d_i	Node degree of n_i.
e_m	Node degree ratio in the mth area original model ($\sum_{n_i \in U_m} d_i / \sum_{i=1}^N d_i$).
d_i^S	Node degree of n_i^S.
e_m^S	Node degree ratio in the mth area small-sized model ($\sum_{n_i^S \in U_m} d_i^S / \sum_{i=1}^{N^S} d_i^S$).

where x_{ij} is equal to

$$x_{ij} = \begin{cases} 1, & \text{if } s_{ij}^{max} \text{ and } s_{i\delta}^{max} \text{ are different stations} \\ & \text{for any } \delta < j, \\ 0, & \text{otherwise.} \end{cases} \quad (2)$$

That is, the number of passengers alighting/boarding at a station is included at most once in (1). Because the total population size cannot be estimated from the number of passengers, the total number of populations in the Tokyo23-day model is set to the same value as Tokyo23-night in (1). However, the impact of the passengers from/to outside 23 wards is considered by p_{ij}^{max}.

5. Compression Algorithm for Designing a Small MAN Model

A large MAN model is effective for evaluating network architecture performance in realistic situations, but it is sometimes unsuitable for simple performance evaluations. In this section, we propose a compression algorithm that shrinks the larger model based on the regional railway information, which again are not used in the extant methods discussed in Sect. 2.1. The proposed compression algorithm can be applied to the original network model in Sect. 3. Table 4 presents a list of variables used in our proposed compression

algorithm.

In the compression algorithm, the number of nodes, N^S, is determined in advance for the small-sized network model. Then, based on regional characteristics, the original large model is divided into M areas so that $M \leq N^S$ is satisfied. For the mth area, a set of nodes in the original network model is denoted as U_m ($m = 1, \cdots, M$), and the number of nodes in U_m is denoted as $|U_m|$. When the node degree of n_i is d_i, the node degree ratio, e_m, of the mth area is defined as $e_m = \sum_{n_i \in U_m} d_i / \sum_{i=1}^N d_i$. Moreover, for the small-sized network model, the node degree ratio, e_m^S, is defined as $e_m^S = \sum_{n_i^S \in U_m} d_i^S / \sum_{i=1}^{N^S} d_i^S$, where n_i^S is the ith node ($i = 1, \cdots, N^S$) in the small-sized network model, and d_i^S is the node degree of n_i^S.

The compression algorithm is applied to the original network model according to the following steps.

B-1) For the mth area ($m = 1, \cdots, M$), $\left\lceil \frac{N^S}{N} |U_m| \right\rceil$ nodes are selected as n_i^S from among U_m so that the total area of the small-sized network model approximates that of the original one. No nodes are selected from an area surrounded by other areas. Then, go to B-2).

B-2) For the mth area ($m = 1, \cdots, M$), the node with the largest degree is selected as n_i^S from U_m. Even if the selected node has already been selected in B-1), another node is not selected. If there are multiple nodes with the largest node degree, a node is randomly selected as n_i^S from among the all, excluding the one selected in B-1). Go to B-3).

B-3) When the number of nodes selected in B-1) and B-2) is smaller than N^S, a node is selected as n_i^S from among the nodes in all areas so that $\sum_{m=1}^M \left| e_m^S - e_m \right|$ is minimized until N^S nodes are selected. On the other hand, when it is larger than N^S, the extra nodes are deleted so that $\sum_{m=1}^M \left| e_m^S - e_m \right|$ is minimized. If N^S nodes are selected, then go to B-4).

B-4) A link is set between any two selected nodes, n_i^S and n_j^S, when a link exists between the two nodes in the original model. Then, go to B-5).

B-5) A link is set between any two selected nodes, n_i^S and n_j^S, when the two nodes are connected within three hops without traversing any selected node, n_k^S, in the original model. Go to B-6).

B-6) If the small-sized model is not a connected graph after two nodes are removed, some nodes and links are changed to provide a connected graph. Then, go to B-7).

B-7) If the designed model is not an appropriate small-sized network model, some nodes and links are changed; go to B-8).

B-8) When multiple links intersect at a point, a link is

deleted until there are no remaining intersections. Then, the algorithm is completed.

From B-1) to B-3), N^S nodes are selected so that the small-sized network model approximates the original network model. If these processes are defined as a minimization problem, N^S nodes can be selected by using software (e.g., CPLEX), a meta-heuristic algorithm (e.g., genetic algorithm), etc. A full search may be available when N and N^S are not very large. Additionally, from B-4) to B-5), links are selected so that the small-sized network model approximates the original one. In B-6), a small-sized network model whose node connectivity is larger than two [50], [51] is designed. In B-8), links between two nodes with longer distances should be deleted. Note that the node connectivity of the small-sized network model may not be larger than two by the processes in B-7) and B-8).

The computational complexity of this algorithm is presented in the Appendix. When M is small (large), the computational complexity increases (decreases).

6. MAN Model with 12 Nodes in Tokyo

In this section, we design a small-sized MAN model with 12 nodes, "Tokyo12", by applying our proposed compression algorithm to Tokyo23. Tokyo12 is also classified into two models, day and night, based on the number of passengers alighting/boarding at each station and the respective population densities.

Figure 5 shows the Tokyo12 MAN model obtained from the Tokyo23 MAN model. Each node is identified by the name of one of the 12 wards located in each ward office building. The correspondence between the ith node, n_i ($i = 1, \cdots, 23$), in Tokyo23 and the ith node, n_i^S ($i = 1, \cdots, 12$), in Tokyo12 is presented in Table 3. To design Tokyo12, N^S and M were set to 12 and 6, respectively, in the compression algorithm. Table 4 shows node sets U_1–U_6 for the six areas determined by the Tokyo Metropolitan Government's Bureau of Industrial and Labor Affairs.
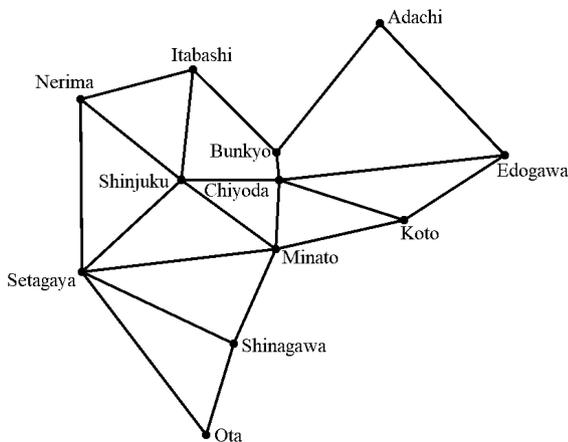
To design Tokyo12 in B-1), we select Minato for U_1,

Koto, Adachi, and Edogawa for U_3, Ota for U_4, Setagaya and Nerima for U_5, and Kita for U_6. No nodes are selected for U_2 because the corresponding area is surrounded by other areas. Then, in B-2), Chiyoda is selected for U_1, Shinjuku for U_2, Sumida for U_3, Shinagawa for U_4, Setagaya for U_5, and Kita for U_6. Note that Setagaya and Kita have already been selected in B-1). Here, we used a full search to select the nodes. B-3) is skipped because the 12 nodes are selected in B-1) and B-2), and the links are set in B-4) and B-5) based on the Tokyo23 model. In B-7), Sumida and Kita are changed to Bunkyo and Itabashi so that Tokyo12 approximates Tokyo23. Moreover, in B-8), the link between Adachi and Koto is deleted. After this algorithm is applied, every link length is set so that the length equals the minimum walking distance

Table 3 Node numbers and names in the Tokyo23 and Tokyo12 MAN models.

Tokyo23	Tokyo12	Name	Population size in Tokyo12
n_1	n_1^S	Chiyoda	$b_1^S = b_1$
n_2	-	Chuo	-
n_3	n_2^S	Minato	$b_2^S = b_2 + b_3$
n_4	n_3^S	Shinjuku	$b_3^S = b_4 + b_{16}$
n_5	n_4^S	Bunkyo	$b_4^S = b_5 + b_6$
n_6	-	Taito	-
n_7	-	Sumida	-
n_8	n_5^S	Koto	$b_5^S = b_7 + b_8$
n_9	n_6^S	Shinagawa	$b_6^S = b_9 + b_{13}$
n_{10}	-	Meguro	-
n_{11}	n_7^S	Ota	$b_7^S = b_{10} + b_{11}$
n_{12}	n_8^S	Setagaya	$b_8^S = b_{12} + b_{15}$
n_{13}	-	Shibuya	-
n_{14}	-	Nakano	-
n_{15}	-	Suginami	-
n_{16}	-	Toshima	-
n_{17}	-	Kita	-
n_{18}	-	Arakawa	-
n_{19}	n_9^S	Itabashi	$b_9^S = b_{17} + b_{19}$
n_{20}	n_{10}^S	Nerima	$b_{10}^S = b_{14} + b_{20}$
n_{21}	n_{11}^S	Adachi	$b_{11}^S = b_{18} + b_{21}$
n_{22}	-	Katsushika	-
n_{23}	n_{12}^S	Edogawa	$b_{12}^S = b_{22} + b_{23}$

Fig. 5 Designed Tokyo12 MAN model.

Table 4 Node set U_m for the compression algorithm.

	Area name	Node name
U_1	Toshin	Chiyoda, Chuo, Minato
U_2	Fuku-toshin	Shinjuku, Bunkyo, Shibuya, and Toshima
U_3	Joto	Taito, Sumida, Koto, Arakawa, and Adachi, Katsushika, Edogawa
U_4	Jonan	Shinagawa, Meguro, Ota
U_5	Josai	Setagaya, Nakano, Suginami, and Nerima
U_6	Johoku	Kita, Itabashi

between two ward office buildings.

In Tokyo12, the size, b_i^S, of the population of n_i^S is derived from the size of the population in Tokyo23, as shown in Table 3. This derivation of b_i^S is determined so that the node distribution of Tokyo12 approximates that of Tokyo23. By using b_i^S, the Tokyo12-day and -night models are designed, as was the case with Tokyo23.

7. Characteristics of the Designed Network Models

In this section, we investigate the characteristics of Tokyo23 and Tokyo12 models shown in Figs. 4 and 5. Information on Tokyo23 and Tokyo12 can be downloaded from [52].

Tables 5 and 6 show the number of nodes, number of links, average node degree, maximum node degree, and minimum node degree of Tokyo23, Tokyo12, JPN48, JPN25, and JPN12. From the comparison with JPN models, we show how the information on regional railway characteristics affects the design of mesh-type MAN models. Node degree is a fundamental network metric that is widely used for network analysis [54]–[56]. Moreover, Table II in [53] shows the characteristics of another 40 network models. The comparison with the 40 models provides researchers with useful information for using our designed models.

From Table 5, we find that the average node degree of Tokyo23 is somewhat larger than those of JPN48 and JPN25, although the number of links in Tokyo23 is not very large. The minimum node degree of Tokyo23 is also larger than those of the other models. Therefore, Tokyo23 is more redundant than JPN48 and JPN25. Among the 40 models in [53], only ITALY with 14 nodes and EON with 19 nodes have higher node degrees than Tokyo23. Table 6 shows that the number of links and average node degree of Tokyo12 are larger than those of JPN12. The maximum node degree of Tokyo12 is also larger than that of JPN12. By contrast, the minimum node degree of Tokyo12 is the same as that of JPN12, unlike the relationship between Tokyo23 and both JPN48 and JPN12. This is because the number of links in Tokyo12 is smaller than that in Tokyo23. The average node degrees of the 38 models apart from ITALY and EON are also smaller than that of Tokyo12. From these results, it is
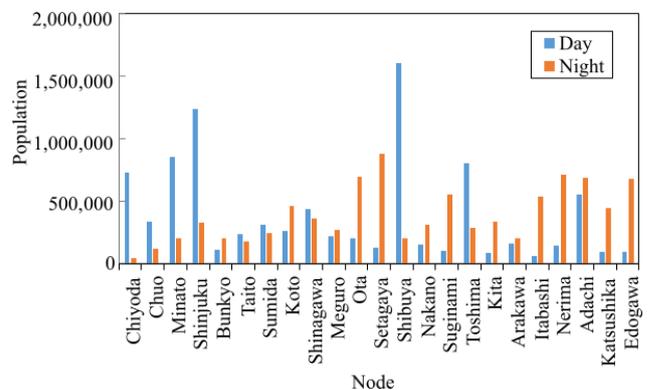
clear that Tokyo23 and Tokyo12 are more appropriate than other models as mesh-type MAN models in Tokyo due to their high node degrees.

Table 7 shows the link length information, which are useful to study routing algorithms, etc., for Tokyo23 and Tokyo12. From this table, we find that the maximum link length of Tokyo23 equals that of Tokyo12. However, the minimum link length of Tokyo23 is smaller than that of Tokyo12. Moreover, the average link length of Tokyo23 is smaller than that of Tokyo12. This is because the number of nodes and links of Tokyo23 is larger than that of Tokyo12, although the position of each node is the same in both models. Table 7 also shows the maximum physical fiber delay, minimum physical fiber delay, and average physical fiber delay, which are derived as 5.0 μs/km based on the link length.
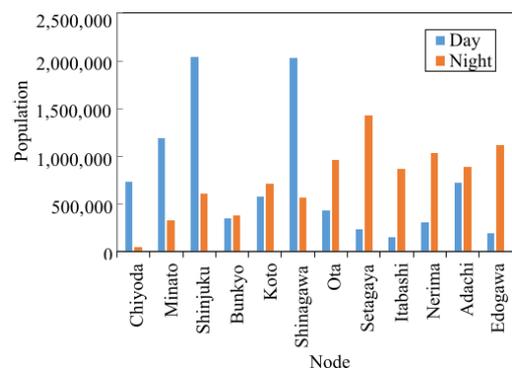
Finally, Figs. 6 and 7 show the population of each node from the day and night models for Tokyo23 and Tokyo12, respectively. From these figures, we find that the difference

Table 7 Link length and physical fiber delay for Tokyo23 and Tokyo12.

	Tokyo23	Tokyo12
Maximum link length [km]	12.4	12.4
Minimum link length [km]	1.9	5.0
Average link length [km]	5.2	7.8
Maximum delay [μs]	62.0	62.0
Minimum delay [μs]	9.5	25.0
Average delay [μs]	26.0	39.0

Fig. 6 Population of each node in Tokyo23.

Table 5 Comparison of Tokyo23, JPN48, and JPN25.

	Tokyo23	JPN48	JPN25
Number of nodes	23	48	25
Number of links	43	82	43
Average node degree	3.74	3.42	3.44
Maximum node degree	5	6	5
Minimum node degree	3	2	2

Table 6 Comparison of Tokyo12 and JPN12.

	Tokyo12	JPN12
Number of nodes	12	12
Number of links	21	17
Average node degree	3.5	2.83
Maximum node degree	5	4
Minimum node degree	2	2

Fig. 7 Population of each node in Tokyo12.

among node populations in the day model is larger than that in the night model. Therefore, the day and night models for Tokyo23 and Tokyo12 are useful performance evaluations in several target situations.

8. Validation of the Designed Network Models

In this section, we consider another network model with 23 nodes, which was designed using communication network information. We then validate our proposed network model design by comparing to this one. Note that the comparison model could not be designed by using the existing approach due to the reasons explained in Sect. 2.1.

It has been reported that the MAN in Tokyo consists of multiple ring networks [57]. Among these, one main ring network approximates the route of the JR Yamanote line, and multiple subring networks are connected to the main one. For each ring network, the nodes are placed in carrier buildings. Figure 8 shows the stations of the JR Yamanote line as red pins and the Nippon Telegraph and Telephone Corporation (NTT) office buildings as blue pins. The main ring network is represented by red pins and a black line, and the seven subring networks are represented by blue pins and black lines so that the Tokyo metropolitan area can be covered.

For the ring networks in Fig. 8, the 23 nodes of Tokyo23 are placed. Each pin is aggregated to a node in the ward to which the pin belong. Then, multiple links are added to improve network redundancy, as follows:

C1: Multiple links are set inside the main ring network based on Tokyo metro optical fiber networks [58].

C2: A link is set between two outermost nodes on adjacent subring networks (e.g., between A and B and between C and D in Fig. 8).

C3: A link is set between two nodes on each subring network (e.g., between E and F in Fig. 8).

Finally, the network model shown in Fig. 9 is designed for the Tokyo metropolitan area. In this model, the yellow links correspond to those of the main ring network, and the red links correspond to links in the seven subring networks. The green links correspond to C1, and the blue links are added to the subring networks to improve network redundancy for C2 and C3.

By comparing Figs. 4 and 9, we find that the number of links in Tokyo23 is greater than that in Fig. 9 because there are no links between Meguro and Ota and between Meguro and Shinagawa in Fig. 9. However, all other links are the same in both models. Therefore, we are convinced that our proposed design algorithm is effective for designing MAN models. Note that the comparative approach used to design Fig. 8 cannot be used to design other MAN models.

9. Conclusions and Future Work

In this paper, we proposed two algorithms that utilize a priori

Fig. 8 One main ring network and seven subring networks in the Tokyo metropolitan area.
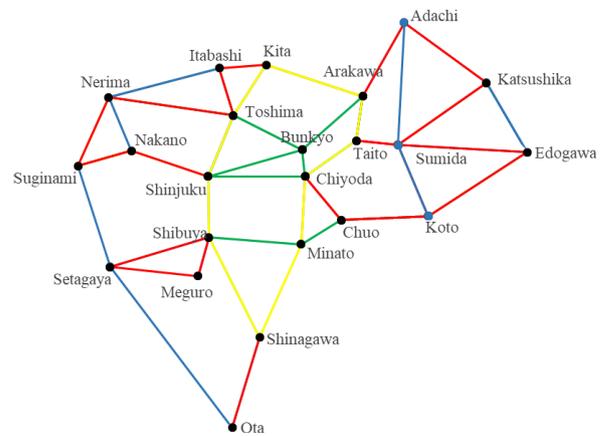
Fig. 9 MAN topology designed using communication network information.

regional railway information to design Tokyo MAN models to accelerate research on B5G in Japan. By using these methods for the Tokyo metropolitan area, we designed Tokyo23 and Tokyo12 MAN models. Then, we constructed four network models, Tokyo23-day, Tokyo23-night, Tokyo12-day, and Tokyo12-night, based on the number of passengers alighting/boarding at each station and the respective population densities. These models were designed using only publicly available information from the Tokyo metropolitan area. We evaluated the characteristics of Tokyo23 and Tokyo12 by comparing them to other models. We also investigated the validity of our proposed design algorithm and the designed models by comparing Tokyo23 with another network models that were designed using communication network information. We are convinced that our proposed algorithm is effective in designing MAN models, and that Tokyo23 is a valid Tokyo MAN model. In a future work, we plan to design MAN models for other major metropolitan areas, such as Osaka and Nagoya, by revising our current algorithms.

Acknowledgments

References

[1] T. Sato, K. Ashizawa, H. Takeshita, S. Okamoto, N. Yamanaka, and E. Oki, "Time estimation of logical optical line terminal migration for elastic lambda aggregation network," IEEE/OSA J. Opt. Commun. Netw., vol.7, no.9, pp.928–941, Sept. 2015.

[2] S. Ibrahim and T. Hashimoto, "Burst-mode enabled optical DC networks: Packet switching and beyond," IEEE Photonics in Switching and Computing, Th3B.3, Sept. 2018.

[3] M. Fiorani, P. Samadi, Y. Shen, L. Wosinska, and K. Bergman, "Flexible network architecture and provisioning strategy for geographically distributed metro data centers," IEEE/OSA J. Opt. Commun. Netw., vol.9, no.5, pp.385–392, May 2017.

[4] H. Nagai, Y. Mori, H. Hasegawa, and K. Sato, "Design and verification of large-scale optical circuit switch using ULCF AWGs for datacenter application," IEEE/OSA J. Opt. Commun. Netw., vol.10, no.7, pp.82–89, July 2018.

[5] Z. Shu, T. Taleb, and J. Song, "Resource allocation modeling for fine-granular network slicing in Beyond 5G systems," IEICE Trans. Commun., vol.E105-B, no.4, pp.349–363, April 2022.

[6] A. Saleh and J. Simmons, "Architectural principles of optical regional and metropolitan access networks," J. Lightw. Technol., vol.17, no.12, pp.2431–2448, Dec. 1999.

[7] P. Arijs, B. Caenegem, P. Demeester, P. Lagasse, W. VanParys, and P. Achten, "Design of ring and mesh based WDM transport networks," Optical Networks Magazine, vol.1, no.3, pp.25–40, July 2000.

[8] N. Antoniades, I. Roudas, G. Ellinas, and J. Amin, "Transport metropolitan optical networking: Evolving trends in the architecture design and computer modeling," J. Lightw. Technol., vol.22, no.11, pp.2653–2670, Nov. 2004.

[9] L. de Sousa and A.C. Drummond, "Metropolitan optical networks: A survey on new architectures and future trends," CoRR, abs/2201.10709, Jan. 2022.

[10] M. Ramachandran, A. Anbiah, and K.M. Sivalingam, "Capacity optimization based on traffic grooming in transport networks," Proc. 2019 IFIP/IEEE Symposium on Integrated Network and Service Management, April 2019, pp.435–441, 2019.

[11] R. Diestel, Graph Theory, Springer Publishing, United States, 2017.

[12] E. Tranos, The Geography of the Internet: Cities, Regions and Internet Infrastructure in Europe, Edward Elgar Publishing, United Kingdom, 2013.

[13] S. Graham and S. Marvin, Telecommunications and the City: Electronic Spaces, Urban Places, Routledge, United Kingdom, 1996.

[14] E.J. Malecki and S.P. Gorman, "Maybe the death of distance, but not the end of geography: the Internet as a network," Worlds of E-Commerce: Economic, Geographical, and Social Dimensions, John Wiley & Sons, United Kingdom, 2001.

[15] M. Dodge and N. Shiode, "Where on Earth is the Internet? An empirical investigation of the geography of Internet real estate," Cities in the Telecommunications Age: The Fracturing of Geographies, Routledge, United Kingdom, 2000.

[16] S.P. Gorman and E.J. Malecki, "The networks of the Internet: An analysis of provider networks in the USA," Telecommunications Pol-

icy, vol.24, no.2, pp.113–134, March 2000.

[17] M.E. O'Kelly and T.H. Grubesic, "Backbone topology, access, and the commercial Internet, 1997–2000," Environment and Planning B: Planning and Design, vol.29, no.4, pp.533–552, Aug. 2002.

[18] T.H. Grubesic and M.E. O'Kelly, "Using points of presence to measure accessibility to the commercial Internet," The Professional Geographer, vol.54, no.2, pp.259–278, Jan. 2002.

[19] E. Tranos, "The topology and the emerging urban geographies of the Internet backbone and aviation networks in Europe: A comparative study," Environment and Planning A: Economy and Space, vol.43, no.2, pp.378–392, Feb. 2011.

[20] E. Tranos and A. Gillespie, "The urban geography of Internet backbone networks in Europe: Roles and relations," J. Urban Technology, vol.18, no.1, pp.30–50, May 2011.

[21] T. Sakano, Y. Tsukishima, H. Hasegawa, T. Tsuritani, Y. Hirota, S. Arakawa, and H. Tode, "A study on a photonic network model based on the regional characteristics of Japan," IEICE Technical Report, PN2013-1, June 2013 (in Japanese).

[22] S. Arakawa, T. Sakano, Y. Tsukishima, H. Hasegawa, T. Tsuritani, Y. Hirota, and H. Tode, "Topological characteristic of Japan photonic network model," IEICE Technical Report, PN2013-2, June 2013.

[23] N. Kitsuwan, H. Tahara, and E. Oki, "Heuristic approach to determining cache node locations in content-centric networks," IEEE Access, vol.6, pp.1542–1549, Dec. 2017.

[24] S. Fujii, Y. Hirota, H. Tode, and K. Murakami, "On-demand spectrum and core allocation for reducing crosstalk in multicore fibers in elastic optical networks," J. Opt Commun. Netw., vol.6, no.12, pp.1059–1071, Dec. 2014.

[25] A. Feldmann, A. Greenberg, C. Lund, N. Reingold, and J. Rexford, "Netscope: Traffic engineering for IP networks," IEEE Netw. Mag., vol.14, no.2, pp.11–19, March/April 2000.

[26] D.A. Maltz, G. Xie, J. Zhan, H. Zhang, G. Hjálmtýsson, and A. Greenberg, "Routing design in operational networks: A look from the inside," ACM SIGCOMM Computer Communication Review, vol.34, no.4, pp.27–40, Oct. 2004.

[27] E. Katz-Bassett, H.V. Madhyastha, V.K. Adhikari, and C. Scott, "Reverse traceroute," Proc. 7th USENIX Symposium on Networked Systems Design and Implementation, April 2010.

[28] N. Spring, R. Mahajan, D. Wetherall, and T. Anderson, "Measuring ISP topologies with rocketfuel," IEEE/ACM Trans. Netw., vol.12, no.1, pp.2–16, Feb. 2004.

[29] CAIDA, "Skitter," http://www.caida.org/tools/measurement/skitter/

[30] D. Feldman and Y. Shavitt, "Automatic large-scale generation of Internet PoP-level maps," Proc. IEEE Globecom 2008, Nov./Dec. 2008, pp.2426–2431, 2008.

[31] H.V. Madhyastha, T. Isdal, M. Piatek, C. Dixon, T. Anderson, A. Krishnamurthy, and A. Venkataramani, "iPlane: An information plane for distributed services" Proc. 7th Symposium on Operating Systems Design and Implementation, Nov. 2006.

[32] Y. Shavitt and N. Zilberman, "A structural approach for PoP geolocation," Proc. IEEE INFOCOM 2010, March 2010.

[33] K. Yoshida, Y. Kikuchi, M. Yamamoto, Y. Fujii, K. Nagami, I. Nakagawa, and H. Esaki, "Inferring PoP-level ISP topology through end-to-end delay measurement," Proc. 6th International Workshop on Passive and Active Network Measurement, pp.35–44, March 2009.

[34] K. Vermeulen, J.P. Rohrer, R. Beverly, O. Fourmaux, and T. Friedman, "Diamond-Miner: Comprehensive discovery of the internet's topology diamonds," 17th USENIX Symposium on Networked Systems Design and Implementation, pp.479–493, Feb. 2020.

[35] W. Willinger, "The Science of Complex Networks and the Internet: Lies, damned lies and statistics," Feb. 2010. http://www.maths.adelaide.edu.au/matthew.roughan/workshops.html

[36] Y. Li, X. Tian, K, Pham, and G. Chen, "A review of network topology inference methods," Proc. Sensors and Systems for Space Applications, XIV, May 2021.

[37] R. Zhang, Y. Li, and X. Li, "Topology inference with network tomography based on t-Test," IEEE Commun. Lett., vol.18, no.6, pp.921–

924, June 2014.

[38] S. Knight, H. Nguyen, N. Falkner, R. Bowden, and M. Roughan, "The internet topology zoo," IEEE J. Sel Areas Commun., vol.29, no.9, pp.1765–1775, Oct. 2011.

[39] R. Bowden, H.X. Nguyen, N. Falkner, S. Knight, and M. Roughan, "Planarity of data networks," Proc. 23rd International Teletraffic Congress, pp.254–261, Sept. 2011.

[40] T.G. Lewis, Network Science - Theory and Applications, John Wiley & Sons, 2009.

[41] P. Erdős and A. Rényi (ER), "On random graphs. I," Publ. Math. Debrecen, vol.6, pp.290–297, 1959.

[42] D. Watts and S. Strogatz, "Collective dynamics of 'small-world' networks," Nature, vol.393, no.6684, pp.440–442, June 1998.

[43] A. Barabási-Albert and R. Albert, "Emergence of scaling in random networks," Science, vol.286, no.5439, pp.509–512, 1999.

[44] R. Gabriel and R. Sokal, "A new statistical approach to geographic variation analysis," Systematic Zoology, vol.18, no.3, pp.259–278, Sept. 1969.

[45] B. Waxman, "Routing of multipoint connections," IEEE J. Sel. Areas Commun., vol.6, no.9, pp.1617–1622, Dec. 1988.

[46] S. Arakawa, T. Takine, and M. Murata, "Analyzing and modeling router-level internet topology and application to routing control," Computer Communications, vol.35, no.8, pp.980–992, May 2012.

[47] A. Fabrikant, E. Koutsoupias, and C. Papadimitriou, "Heuristically optimized trade-offs: A new paradigm for power law in the internet," Proc. 29th International Colloquium on Automata, Languages, and Programming, pp.110–122, July 2002.

[48] https://www.ieice.org/cs/pn/jpn/JPNM/JPNM_v20161013sn(E).zip

[49] S. Jendrol', J. Miškuf, R. Soták, and E. Skrabal'áková, "Rainbow faces in edged colored plane graphs," J. Graph Theory, vol.62, no.1, pp.84–99, Sept. 2009.

[50] M.R. Henzinger, S. Rao, and H.N. Gabow, "Computing vertex connectivity: New bounds from old techniques," J. Algorithms, vol.34, no.2, pp.222–250, Feb. 2000.

[51] S. Latifi, M. Hegde, and M. Naraghi-Pour, "Conditional connectivity measures for large multiprocessor systems," IEEE Trans. Comput., vol.43, no.2, pp.218–222, Feb. 1994.

[52] https://www.ieice.org/cs/pn/eng/ (After the review process, we will update URL. During this review process, reviewers can download a zip file from http://ginyu.fuis.u-fukui.ac.jp/members/takuji-t/PN/ [ID: PN, PASS: topology].)

[53] S.K. Routray, G. Sahin, J.R. Ferreira da Rocha, and A.N. Pinto, "Statistical analysis and modeling of shortest path lengths in optical transport networks," IEEE/OSA J. Lightw. Technol., vol.33, no.13, pp.2791–2801, July 2015.

[54] Network analysis of protein interaction data, https://www.ebi.ac.uk/training/online/courses/network-analysis-of-protein-interaction-data-an-introduction/

[55] W. Si, B. Mburano, W.X. Zheng, and T. Qiu, "Measuring network robustness by average network flow," IEEE Trans. Netw. Sci. Eng., vol.9, no.3, pp.1697–1712, May/June 2022.

[56] Z. Wan, Y. Mahajan, B.W. Kang, T.J. Moore, and J. Cho, "A survey on centrality metrics and their network resilience analysis," IEEE Access, vol.9, pp.104773–104819, July 2021.

[57] JANOG8 Meeting Program, https://www.janog.gr.jp/meeting/janog8/log/okapon-darkfiber.txt (in Japanese).

[58] https://www.tokyometro.jp/corporate/business/optical_fiber/pdf/network.pdf

Appendix: Computational Complexity

We consider the computational complexity of the proposed design algorithm in Sect. 3 in the case where a metropolitan area network (MAN) model with N nodes is designed. Because the number of railway lines for node n_i is L_i

$(i = 1, \cdots, N)$, $r_{i\delta}$ and $r_{i\eta}$ are selected from among $_{L_i}C_2 = \frac{L_i(L_i-1)}{2}$ pairs of railway lines in A-2). In A-3), two links are set for each node; hence, the number of processes is $2N$. The processes in A-2) and A-3) are repeated N times from A-1) to A-4). Moreover, in A-5), a maximum of $2N$ links are checked. Finally, two links are checked for each node whose node degree is the highest in A-6). Consequently, the computational complexity is given by

$$O\left(N\left(\frac{L_i(L_i-1)}{2} + 2N\right) + 2N + 2N\right)$$

$$= \begin{cases} O(NL_i^2), & \text{if } \frac{L_i(L_i-1)}{2} > 2N, \\ O(N^2), & \text{otherwise.} \end{cases} \quad (A\cdot 1)$$

Next, we consider the computational complexity of the compression algorithm in Sect. 5 when the small-sized network model with N^S nodes is designed from the original network model with N nodes ($N^S < N$). Next, to derive the computational complexity, we assume that the number of links is K and K^S in the original and small-sized network models, respectively.

In the compression algorithm, the minimization problem is solved in B-3). In most cases, the computational complexity depends on the algorithm used to derive the minimization problem. We next consider a special case in which the computational complexity from B-1) to B-8), excluding B-3), is larger than that of the algorithm for the minimization problem. Moreover, we assume that $N - N^S$ is larger than three; that is, more than three nodes are deleted from the original network model to design the small-sized version.

In B-1), $\left\lceil \frac{N^S}{N}|U_m| \right\rceil$ nodes must be selected from among the $|U_m|$ nodes for the mth area to calculate the total area for all node combinations. When $\frac{N^S}{N}$ is denoted as α ($0.5 < \alpha < 1.0$), and $\alpha|U_m|$ is an integer, the number of calculations for the total area is given by $\prod_{m=1}^{M} |U_m|C_{\alpha|U_m|}$. Moreover, if $|U_m|$ is equal to $\frac{N}{M}$, regardless of m, the computational complexity in B-1) is given by $O((\frac{N}{M})^{(\frac{N}{M} - \alpha\frac{N}{M})M})$. Then, in B-2), most of the αN nodes, where αN is equal to N^S, are checked to select the node with the largest node degree for each area. In B-4), $_{\alpha N}C_2$ pairs of nodes are checked in the original network model to set links between any two nodes, and the computational complexity is $O(\alpha^2 N^2)$. In B-5), following the Dijkstra algorithm, whose computational complexity, $O((N - \alpha N + K)\log(N - \alpha N))$, is used in the original network model without αN nodes, the number of hops is checked for $_{\alpha N}C_2$ pairs of nodes. Therefore, the computational complexity is $O((N - \alpha N + K)\log(N - \alpha N) + \alpha^2 N^2)$. In B-6), a connected network is checked $\alpha^2 N^2$ times because the number of pairs of deleted nodes is $_{\alpha N}C_2$. If the breadth-first search algorithm is used in this process, the computational complexity is $O(\alpha^2 N^2(\alpha N + \beta K))$, where βK is equal to K^S ($0 < \beta < 1$). At most, αN nodes and βK links are checked in B-7), and $\beta^2 K^2$ pairs of links are checked in B-8). Consequently, the computational complexity is given by

$$O\left(\left(\frac{N}{M}\right)^{(N-\alpha N)} + \alpha N + \alpha^2 N^2 \right.$$
$$+ (N - \alpha N + K)\log(N - \alpha N) + \alpha^2 N^2$$
$$+ \alpha^2 N^2(\alpha N + \beta K) + \alpha N + \beta K + \beta^2 K^2\Big)$$
$$= O\left(\left(\frac{N}{M}\right)^{(N-\alpha N)}\right) = O\left(\left(\frac{N}{M}\right)^{(N-N^S)}\right), \qquad (A \cdot 2)$$

where N and N^S are smaller than K and K^S, respectively.

Takuji Tachibana received the B. Eng. degree from the Department of Systems Engineering, Nagoya Institute of Technology, Japan, in 2000. He received M. Eng. and Dr. Eng. degrees from the Department of Information Systems, Graduate School of Information Science, Nara Institute of Science and Technology, Japan in 2001 and 2004, respectively. From 2004 to 2006, he was an expert researcher in the Information and Network Systems Department, National Institute of Information and Communications Technology, Japan. From 2006 to 2011, he was an assistant professor in the Department of Information Systems, Graduate School of Information Science, Nara Institute of Science and Technology, Japan. From 2011 to 2018, he was an associate professor in the Graduate School of Engineering, University of Fukui, Japan. Since 2019, he has been a professor in the Graduate School of Engineering, University of Fukui, Japan. He is a member of the IEEE, Institute of Electronics, Information and Communication Engineers (IEICE) and the Operations Research Society of Japan.

Yusuke Hirota received B.E., M.E., and Ph.D. degrees from Osaka University, Osaka, Japan, in 2004, 2006, and 2008, respectively. He joined the Department of Information Networking, Graduate School of Information Science and Technology, Osaka University, in 2008 as an assistant professor. Since 2017, he has worked with the National Institute of Information and Communications Technology (NICT), Tokyo, Japan. His research interests include all-optical networking, optical fiber communication systems, multimedia streaming systems, and autonomous networks. Dr. Hirota is a member of IEEE, Optica, and IEICE.
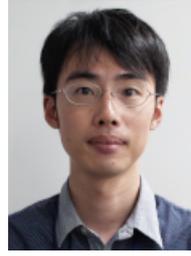
Keijiro Suzuki received his B.E. and M.E. degrees from the Department of Electrical and Electronic Engineering, Shizuoka University, Hamamatsu, Japan, in 2004 and 2006, respectively. After spending two years at Sumitomo Osaka Cement Co., Ltd., he entered the Department of Electrical and Computer Engineering, Yokohama National University (YNU), Yokohama, Japan, in 2008 and was awarded the Research Fellowship for Young Scientists from JSPS. He received his Ph.D. degree from YNU in 2011. After spending one year at YNU as a postdoctoral fellow, he joined the National Institute of Advanced Industrial Science and Technology (AIST), Tsukuba, Japan, in 2012. He is a member of Optica, IEEE Photonics Society, IEICE, and JSAP. His research interests include photonic integrated circuits, nanophotonics, and nonlinear optics.

Takehiro Tsuritani received M.E. and Ph.D. degrees in electronics engineering from Tohoku University, Miyagi, Japan, in 1997 and 2006, respectively. He joined the Kokusai Denshin Denwa (KDD) Company, Limited (currently KDDI Corporation), Tokyo, Japan, in 1997. Since 1998, he has been with their Research and Development Laboratories (currently KDDI Research, Inc.), and has been engaged in research on high-capacity long-haul wavelength division-multiplexed (WDM) transmission systems and dynamic photonic networking. He is currently an executive director at KDDI Research Inc. He is a senior member of the IEEE and a fellow of IEICE. He was a recipient of the Best Paper Award at OECC2000, COIN2014, OECC/PS2016, and OECC2018.

Hiroshi Hasegawa received his B.E., M.E., and D.E. degrees in electrical and electronic engineering from the Tokyo Institute of Technology in 1995, 1997, and 2000, respectively. He is currently a professor at the Graduate School of Engineering, Nagoya University, where he was an associate professor from 2005 to 2019. Before joining Nagoya University, he was an assistant professor at the Tokyo Institute of Technology from 2000 to 2005. His current research interests include network/node architectures, devices, design and control of photonic networks, multidimensional digital signal processing, and time–frequency analysis. Dr. Hasegawa is a senior member of IEICE and a member of IEEE.